RSC Advances

PAPER

View Article Online
View Journal | View Issue

Cite this: *RSC Adv.*, 2026, **16**, 29490

A ready-to-use deep eutectic solvent-immersed polypropylene fabric cap microextraction strategy for nonsteroidal anti-inflammatory drugs analysis in plasma: a proof-of-concept study

Jin-Yue Dong,[ab] Rong-Jie Wang,[bc] Xiao-Bei Yang,[d] Ying-Fei Liu,[e] Qing Ran*[a] and Di Chen *[ef]

The determination of non-steroidal anti-inflammatory drugs (NSAIDs) is important for pharmaceutical analysis and bioanalytical research. In this study, a proof-of-concept deep eutectic solvent-immersed polypropylene fabric cap microextraction (DES-PPF-CME) method was developed for the determination of NSAIDs in plasma. The proposed device integrates polypropylene fabric immobilized with a hydrophobic deep eutectic solvent (DES) into a disposable centrifuge tube cap, enabling analyte extraction *via* simple shaking without the need for complex instrumentation. This configuration represents a new format of supported liquid membrane extraction, offering a simplified, ready-to-use workflow that is amenable to batch processing. Under optimized conditions, including 18 μL of DES composed of methyltrioctylammonium bromide and decanoic acid at a molar ratio of 1 : 3, a sample pH of 5.3, an extraction time of 22 min, and desorption with 0.2 mL of acetonitrile for 3 min, extraction recoveries of 59.6–84.4% were obtained. When coupled with high-performance liquid chromatography–ultraviolet detection, the method demonstrated acceptable linearity ($R^2 \geq 0.9839$), low limits of detection (1.1–19.7 ng mL^{-1}), and satisfactory precision (RSD ≤ 8.6%) in spiked plasma samples. These initial findings suggest that the disposable and easy-to-operate DES-PPF-CME configuration is a promising platform for further development toward the routine analysis of NSAIDs in complex biological matrices.

Received 28th March 2026
Accepted 22nd May 2026

DOI: 10.1039/d6ra02568d

rsc.li/rsc-advances

1. Introduction

Non-steroidal anti-inflammatory drugs (NSAIDs) are among the most widely prescribed medications globally for pain management and inflammation control.[1,2] Although routine blood monitoring is generally not required due to their relatively wide therapeutic windows, accurate pharmacokinetic assessment in plasma is valuable in specific clinical scenarios, such as preventing toxicity in patients with altered metabolism, monitoring high-dose therapies, or conducting bioequivalence studies.[3] However, the reliable determination of NSAIDs in biological matrices remains a challenging task due to the low concentrations of analytes, the complexity of plasma composition, and the presence of potential matrix interferences. Conventional sample preparation methods, such as liquid–liquid extraction (LLE) and solid-phase extraction (SPE), are often labor-intensive, require large volumes of organic solvents, and rely on complex operational steps, limiting their applicability in routine or high-throughput clinical analyses.[4,5]

To address these limitations, microextraction techniques, including dispersive liquid–liquid microextraction (DLLME) and solid-phase microextraction (SPME), have been developed to improve analytical sensitivity.[6–8] In particular, SPME has evolved into a variety of device configurations to meet different application needs, such as fiber-based, in-tube, in-tip, and thin-film formats.[9] Despite these advancements, a major bottleneck restricting the wider adoption of these methods is their difficulty in automation and batch processing. For instance, drop-based methods (*e.g.*, SDME) involve unstable micro-droplets that require delicate, sequential manual operation, while fiber-based methods (*e.g.*, SPME) often utilize fragile fibers that are prone to breakage and difficult to array for parallel

[a]*Department of Ultrasound Medicine, The Second Affiliated Hospital of Zhengzhou University, Zhengzhou 450014, China. E-mail: ranqing1971@163.com*

[b]*The Second Clinical College of Zhengzhou University, Zhengzhou 450014, China*

[c]*Department of Reproductive Medicine, The Second Affiliated Hospital of Zhengzhou University, Zhengzhou 450014, China*

[d]*Clinical Trial Institution for Drugs of Pharmacy Department, The Second Affiliated Hospital of Zhengzhou University, Zhengzhou 450014, China*

[e]*Henan Key Laboratory of Nanomedicine for Targeting Diagnosis and Treatment, School of Pharmaceutical Sciences, Zhengzhou University, Zhengzhou 450001, China. E-mail: dichen@zzu.edu.cn*

[f]*Children's Hospital Affiliated to Zhengzhou University, Zhengzhou University, Zhengzhou, 450018, China*

extraction. These physical limitations make existing microextraction approaches hard to automate, strictly limiting sample throughput and increasing the workload for laboratory personnel. Therefore, there is a growing demand for a robust extraction platform that is structurally amenable to high-throughput processing and can simplify the workflow without the need for specialized equipment.

Equally critical is the selection of the extraction solvent, particularly concerning operator safety and workplace comfort. Traditional hydrophobic solvents used in liquid-phase microextraction, such as *n*-octanol, chloroform, or toluene, are highly volatile and often emit pungent, irritating odors, posing potential health risks to operators during daily routine analysis.[10,11] In contrast, deep eutectic solvents (DESs) have emerged as superior alternatives due to their negligible vapor pressure, non-flammability, and lack of irritating odors, offering a significantly more operator-friendly working environment. Moreover, the physicochemical properties of DESs can be tailored by adjusting the hydrogen bond donors and acceptors to achieve optimal selectivity for target analytes.[12] However, the direct application of DESs faces a practical hurdle: their inherent high viscosity. This characteristic makes dispersion difficult and phase separation slow in conventional liquid–liquid modes, complicating the retrieval of the extraction phase and hindering the development of automated or rapid procedures.[13] Even in DES-based DLLME methods, where DESs serve as extraction solvents, the procedures generally still require a dispersion step followed by centrifugation for phase separation,[14] which limits their compatibility with high-throughput workflows.

In this proof-of-concept study, a facile and disposable deep eutectic solvent-immersed polypropylene fabric cap microextraction (DES-PPF-CME) strategy was developed to address these challenges by combining high throughput, operational convenience, and operator safety. The core innovation of this work is the integration of a DES-impregnated polypropylene fabric directly into a disposable centrifuge tube cap, creating a new ready-to-use, cap-type format of supported liquid membrane extraction. Unlike previously reported DES-based microextraction systems that typically rely on dispersion and centrifugation, or conventional polypropylene/fabric-supported formats that require manual handling of the extraction phase,[15,16] the proposed cap-type supported liquid membrane format physically confines the extraction solvent within the cap. Simple inversion or shaking of the closed tube allows the aqueous sample to contact the DES-loaded membrane, and after extraction, the phases are instantaneously separated when the tube is returned to an upright position. This design allows the simultaneous processing of multiple samples and improves compatibility with batch processing and potential automation. Factors influencing extraction performance, including DES composition, sample pH, and desorption conditions, were systematically investigated. The proposed DES-PPF-CME method provides a practical, user-friendly, and efficient solution, with promising potential for further development toward routine bioanalysis of NSAIDs.

2. Experimental section

2.1. Chemicals and reagents

Sulindac (SLD, ≥99%), dipotassium hydrogen phosphate (K_2HPO_4) and phosphoric acid (H_3PO_4) were purchased from Aladdin Biochemical Technology Co., Ltd (Shanghai, China). Loxoprofen (LOX, ≥98%), naproxen (NPX, ≥99%), flurbiprofen (FBP, ≥98%), diclofenac sodium (DCF, ≥98%), and ibuprofen (IBU, ≥99%) were purchased from Titan Technology Co., Ltd (Shanghai, China), chemical information of target analytes is listed in Table S1. HPLC-grade methanol (MeOH), ethanol (EtOH), acetonitrile (ACN), and acetone were purchased from Aladdin Biochemical Technology Co., Ltd (Shanghai, China). Ultrapure water (H_2O) was obtained from a Milli-Q water purification system (Millipore, Billerica, MA, USA). MTOAB (≥98%) was obtained from Adamas Reagent Technology Co., Ltd (Shanghai, China). *n*-Octanol (≥99%) and *n*-decanol (≥97%) were all purchased from Energy Chemical Industrial Inc. (Shanghai, China). Octanoic acid (≥99%) and decanoic acid (≥99%) were purchased from Shandong Keyuan Biochemical Co., Ltd (Shandong, China).

Polypropylene fabrics, commercially marketed as polypropylene nonwoven filters, were obtained from Tiantai Nanhe Filtration Material Co., Ltd (Zhejiang, China). These industrial-grade materials are primarily designed for oil filtration and are available in pore sizes of 25, 50, 100, 150, and 300 μm.

2.2. Solution preparation

Individual stock solutions of the six NSAIDs (SLD, LOX, NPX, FBP, DCF, and IBU) were prepared in MeOH at a concentration of 5.0 mg mL^{-1}. A mixed standard solution containing 0.5 mg mL^{-1} of each analyte was prepared by diluting the individual stock solutions with MeOH. These solutions were stored at −20 °C and renewed weekly. Working solutions at the desired concentrations were prepared by serial dilution with H_2O.

Phosphate-buffered saline (PBS, 20 mM) was prepared by dissolving K_2HPO_4 in H_2O, and the pH was subsequently adjusted to the desired values using H_3PO_4. The pH measurements were performed using a Leici PHS-3E pH meter (Shanghai Instrument, China).

2.3. Sample collection and pretreatment

Blank plasma specimens were obtained from drug-free healthy donors.[17,18] Specifically, blood was collected in heparinized tubes to prevent coagulation, and then centrifuged at 5000 rpm for 10 min at 4 °C to separate the plasma. To minimize variability due to a single plasma source, a pooled blank plasma sample was prepared by mixing plasma from different individuals. This pooled sample was used as the blank plasma for all subsequent analyses.

Plasma samples were stored at −80 °C in the dark for up to three months. Prior to analysis, the samples were thawed at room temperature (~20 °C). Spiked plasma samples were prepared by adding specific amounts of NSAIDs to blank plasma to achieve target concentration levels. To reduce viscosity and control pH, the plasma was diluted with PBS.

Specifically, 100 μL of plasma was diluted tenfold with PBS (20 mM, pH 5.3), resulting in a total volume of 1 mL. The resulting solution was then ready for subsequent analysis.

2.4. Fabrication of the DES-PPF-CME device

The DESs were synthesized following previously reported methods.[19,20] Briefly, the hydrogen bond acceptor (HBA), MTOAB, was mixed with various hydrogen bond donors (HBDs), including *n*-octanol, *n*-decanol, octanoic acid, and decanoic acid, in specific molar ratios (*e.g.*, 1 : 2 or 1 : 3). The mixtures were stirred using a magnetic stirrer at 60 °C and 200 rpm for 15 min until homogeneous, transparent liquids were obtained.

For the fabrication of the extraction device, the caps of 1.5 mL centrifuge tubes served as the platform. Commercially purchased PPF sheets were used as the support material. Circular discs with a diameter of 8 mm and a thickness of approximately 2 mm were punched from the PPF sheets and inserted into the inner cavity of the caps, where they were tightly secured by mechanical fitting to ensure stable and snug fixation. Subsequently, 18 μL of the prepared DES was accurately dispensed onto the center of the circular PPF disc. Facilitated by the excellent lipophilicity of the PP material, the DES uniformly permeated the fiber matrix, thereby yielding the completed DES-PPF-CME device. The prepared devices were intended for single use to avoid cross-contamination and ensure reproducibility. After fabrication, the devices were sealed in plastic bags and stored at room temperature prior to use.

2.5. DES-PPF-CME procedure

As illustrated in Fig. 1, the extraction procedure was performed as follows: first, 1 mL of the diluted sample solution was transferred into the fabricated DES-PPF-CME device. To initiate extraction, the tube was inverted to ensure full contact between the DES-immersed PPF and the sample solution. The extraction was conducted in a multi-well shaker with a constant agitation speed of 1000 rpm for 22 min. Subsequently, the cap was removed and transferred to a new centrifuge tube pre-filled with 0.2 mL of ACN. Facilitated by the excellent miscibility between the DES and ACN, desorption was performed by shaking the inverted tube at 1000 rpm for 3 min. Finally, the desorption solution containing the enriched analytes was collected for subsequent analysis *via* HPLC-UV.

2.6. Analytical conditions

Chromatographic analysis was performed on an Agilent 1200 Infinity HPLC system (USA) coupled with a UV detector. Separation was achieved using a ZORBAX SB-C18 column (4.6 mm × 250 mm, 5 μm) maintained at 30 °C. The mobile phase consisted of H_2O and ACN (45 : 55, v/v), delivered isocratically at a flow rate of 1.0 mL min^{-1}. The total run time was 20 min, with a detection wavelength of 230 nm and an injection volume of 10 μL.

3. Results and discussions

3.1. Experimental design

This study aims to develop a facile, disposable, and ready-to-use microextraction strategy by integrating the extraction phase directly into the cap of a standard centrifuge tube. In this design, a circular PPF disc serves as the solid support to immobilize the hydrophobic DES within the cap cavity. Due to the inherent lipophilicity and hydrophobicity of the PPF, the viscous DES is spontaneously retained within the porous network, ensuring a stable extraction interface.

The proposed DES-PPF-CME device simplifies the sample preparation workflow into a straightforward "cap-and-shake" process. Unlike traditional liquid-phase microextraction

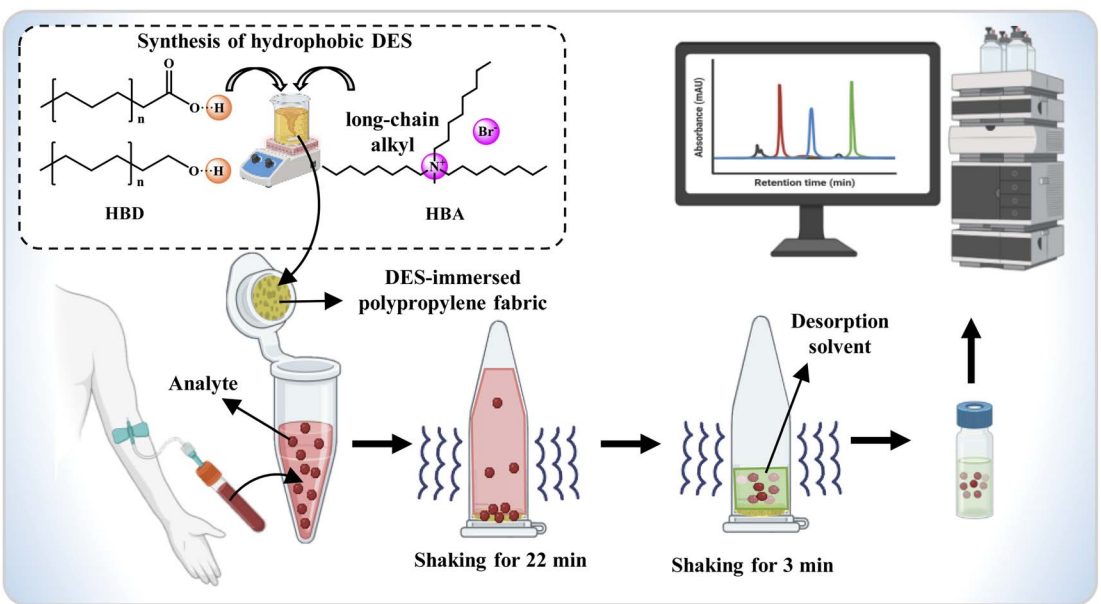

Fig. 1 Schematic illustration of the DES-PPF-CME strategy.

techniques that require complex manual operations, this method involves simply loading the sample solution followed by agitation for extraction and desorption, eliminating the need for centrifugation or precision-dependent steps. Furthermore, this robust design, combined with the simple agitation mechanism, facilitates high-throughput analysis, as a large number of samples can be processed simultaneously using a standard multi-well shaker. Benefiting from the low volatility of DESs, the extraction caps can also be pre-fabricated and stored, enabling a "prepare-in-advance, use-on-demand" strategy.

3.2. Characterization of PPF and DES

The surface morphology and microstructure of the PPF were characterized to assess its suitability as a solid support for the DES. Macroscopically, the PPF presents a uniform, dense, nonwoven white texture with good structural integrity (Fig. 2A). Scanning electron microscopy (SEM) analysis (Fig. 2B) reveals that the PPF consists of a tightly entangled network of fine polypropylene filaments, with diameters ranging from approximately 3 to 5 μm. Under higher magnification (Fig. 2C), the fibers display relatively smooth surfaces arranged in a random orientation, creating a complex three-dimensional scaffold with abundant interstitial voids. This highly porous network provides sufficient internal volume and capillary channels, facilitating the rapid uptake and stable immobilization of the hydrophobic DES.

The physicochemical properties of the optimized DES (MTOAB and decanoic acid at a 1 : 3 molar ratio) were also investigated. As shown in Fig. 2D, the prepared DES is a homogeneous, transparent, light-yellow liquid at room temperature, indicating the successful formation of a stable eutectic phase without precipitation. To evaluate its fluidity, the viscosity–temperature profile was measured (Fig. 2E). The DES exhibits a relatively high viscosity of approximately 307 mPa s at 25 °C, which decreases exponentially as the temperature rises, eventually stabilizing above 120 °C. This high intrinsic viscosity at room temperature confirms that the DES is unsuitable for conventional dispersive methods due to slow mass transfer but is ideal for the proposed DES-PPF-CME method, where the PPF support mitigates the need for solvent dispersion.

Furthermore, the formation mechanism of the DES was verified using FT-IR spectroscopy (Fig. 2F). The spectrum displays broad absorption bands between 3300 and 2500 cm^{-1}, corresponding to the O–H stretching vibrations of the carboxylic acid group in decanoic acid involved in hydrogen bonding. Strong absorption peaks at 2920 and 2850 cm^{-1} are attributed to the C–H stretching vibrations of the alkyl chains. Notably, the C═O stretching vibration appears in the 1700–1715 cm^{-1} region. The specific shifts and broadening of these characteristic peaks, along with the presence of C–N and C–O bands, confirm the establishment of a robust hydrogen-bond network between the halide anion of the salt (MTOAB) and the carboxylic acid donor (decanoic acid), validating the successful synthesis of the deep eutectic solvent.

3.3. Preliminary evaluation of the effectiveness of DES-PPF-CME

The extraction performance and chromatographic cleanliness of the DES-PPF-CME device were preliminarily evaluated using aqueous solutions spiked with six NSAIDs at a concentration of 2 μg mL^{-1}. For reference, standard solutions at the same concentration were analyzed to establish the retention times of each analyte (Fig. 3a). In addition, control experiments were performed using a bare PPF cap without DES loading (Fig. 3b), as well as a blank aqueous sample processed with the DES-PPF-

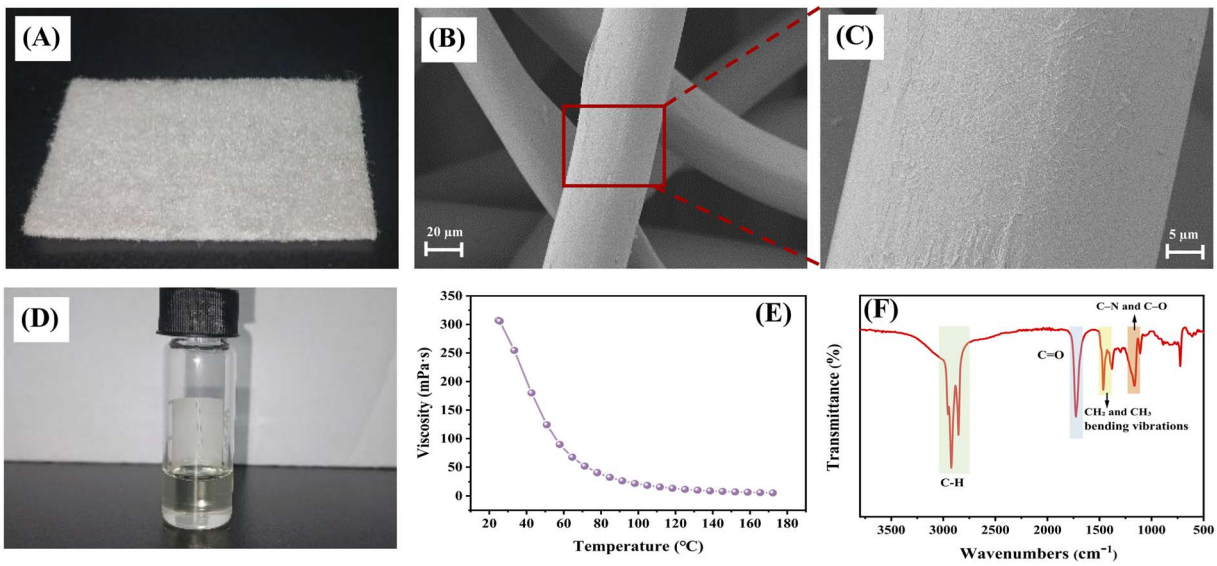

Fig. 2 Characterization of PPF and DES: (A) macroscopic appearance of PPF, (B) SEM image showing fiber network of PPF (500×); (C) high-magnification SEM image displaying fiber surface morphology (2000×), (D) visual appearance of the synthesized DES (MTOAB/decanoic acid, molar ratio 1 : 3), (E) viscosity–temperature profile of the DES, and (F) FT-IR spectrum of the DES.

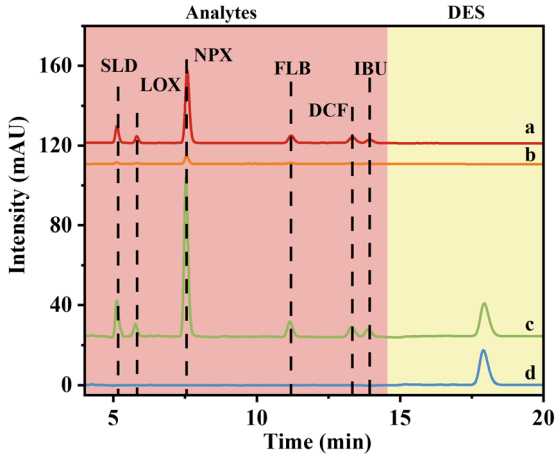

Fig. 3 HPLC-UV chromatograms of six NSAIDs under different experimental conditions: (a) standard solution (2 μg mL^{-1}), (b) spiked sample (2 μg mL^{-1}) extracted using a bare PPF cap without DES, (c) spiked sample (2 μg mL^{-1}; theoretical enrichment factor of 5) extracted using the DES-immersed PPF cap, and (d) blank sample processed with the DES-immersed PPF cap. Abbreviations of NSAIDs: SLD: Sulindac, LOX: Loxoprofen, NPX: Naproxen, FBP: Flurbiprofen, DCF: Diclofenac sodium, IBU: Ibuprofen.

CME device to assess potential background interference (Fig. 3d).

As shown in Fig. 3c, all six NSAIDs were successfully extracted by the DES-immersed PPF cap, and their retention times were in excellent agreement with those of the corresponding standards, indicating that the extraction process did not alter chromatographic behavior. Moreover, the peak responses obtained after extraction were consistent with the expected signal intensity for a 2 μg mL^{-1} solution under the applied enrichment conditions, confirming the effective enrichment capability of the DES-PPF-CME device. In contrast, extraction using the bare PPF cap without DES (Fig. 3b) resulted in only weak analyte signals, demonstrating that polypropylene fibers alone possess limited adsorption ability. Notably, the peak intensities obtained with the DES-loaded PPF cap were more than one order of magnitude higher than those achieved with bare PPF, highlighting the key role of DES in analyte extraction. The blank extract processed with the DES-PPF-CME device (Fig. 3d) exhibited a clean chromatographic baseline, with no detectable interference peaks within the retention windows of the target NSAIDs. A single late-eluting peak at approximately 17.6 min was observed and attributed to the DES itself, which did not overlap with any analyte signals. Importantly, this clean background was achieved without any pre-washing or conditioning of the PPF, underscoring the intrinsic cleanliness and practical convenience of the device.

Throughout the shaking-assisted extraction process, no detachment or displacement of the PPF disc from the centrifuge tube cap was observed, confirming the mechanical robustness and operational stability of the DES-PPF-CME configuration. Collectively, these results demonstrate that the proposed device enables efficient extraction of NSAIDs with minimal background interference and reliable structural integrity, providing a solid foundation for subsequent optimization and application in complex biological matrices.

3.4. Single-factor effects on extraction performance

Single-factor optimization experiments were systematically conducted to maximize the extraction recovery of the NSAIDs using the DES-PPF-CME method. Key parameters were investigated, including DES composition (components and molar ratio), DES volume, PPF pore size, sample solution pH, extraction time, as well as desorption solvent type, volume, and time. All experiments were performed in triplicate ($n = 3$), and the mean extraction recovery was used as the evaluation criterion to identify the optimal conditions. The initial experimental conditions were established as follows: 10 μL of DES (MTOAB : decanoic acid, 1 : 2 molar ratio) was loaded onto the PPF cap. Extraction was performed on 1.0 mL of sample solution (2.0 μg mL^{-1} of NSAIDs) at 1000 rpm for 15 min, followed by desorption with 200 μL of ACN for 3 min.

3.4.1. DES composition and volume. The composition of the DES and the molar ratio of HBA to HBD were systematically evaluated, as these factors determine the physicochemical properties of the solvent (*e.g.*, polarity and viscosity) and consequently influence the extraction efficiency. MTOAB was selected as the HBA, while fatty acids and alcohols with varying carbon chain lengths were investigated as HBDs.

The effect of the HBD type on the extraction recovery is illustrated in Fig. 4A. All four synthesized DESs exhibited the capability to extract the six NSAIDs. Although the differences in extraction recoveries were not statistically significant, the DES prepared with decanoic acid yielded slightly superior extraction performance and was therefore selected for further optimization.

Subsequently, the molar ratio of HBA to HBD (MTOAB : decanoic acid) was optimized by evaluating ratios of 1 : 1, 1 : 1.5, 1 : 2, 1 : 2.5, and 1 : 3. As shown in Fig. 4B, the extraction recovery remained relatively constant across the tested ratios. However, the viscosity of the DES decreased significantly as the proportion of decanoic acid increased. A lower viscosity is critical for practical operation, as it allows for easier and more accurate handling when using a micropipette. Consequently, the 1 : 3 molar ratio was chosen for subsequent experiments to ensure operational convenience and precise volume transfer.

Finally, the volume of DES was optimized in the range of 10–50 μL to balance enrichment efficiency with solvent consumption. As observed in Fig. 4C, the extraction recovery increased significantly as the volume rose from 10 μL to 20 μL, attributed to the increased availability of extraction sites. Beyond 20 μL, the extraction recovery reached a plateau, indicating that the extraction equilibrium had been achieved. Therefore, 20 μL of DES was selected as the optimal volume for the following experiments.

3.4.2. Sample solution pH. The pH of the sample solution is a critical parameter, as it influences not only the existing state of the analytes but also the stability of the DES and the interactions between them. In designing the extraction system, the predominant retention mechanism was initially anticipated to

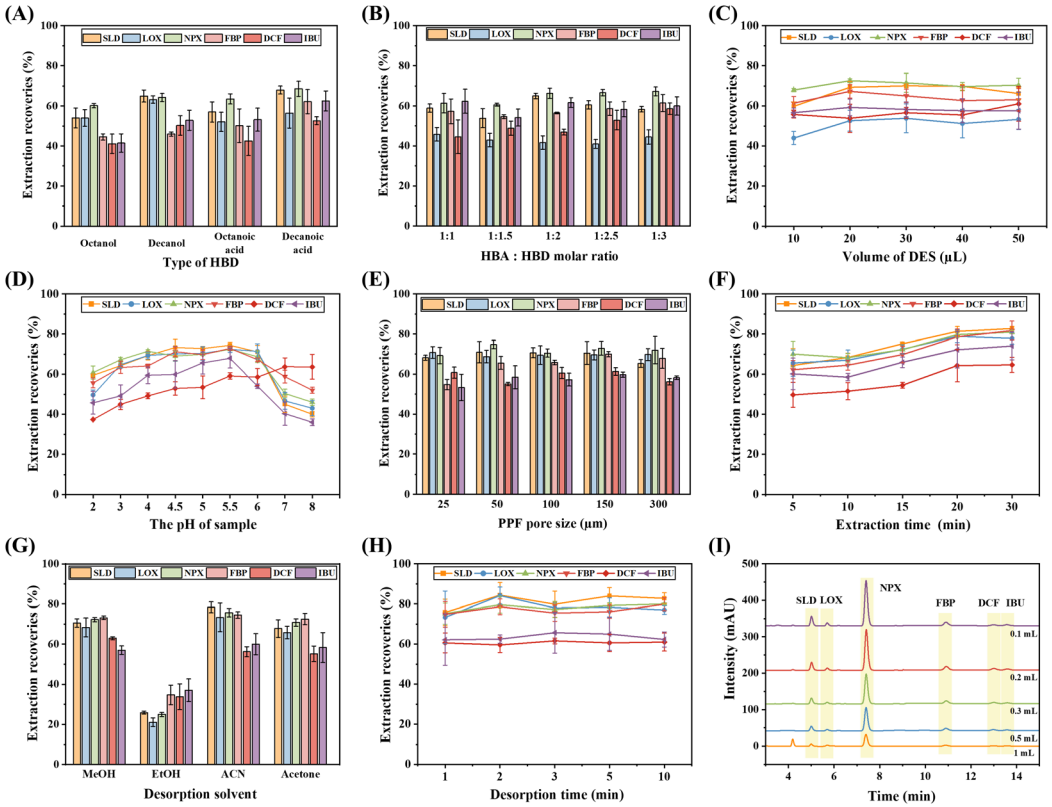

Fig. 4 Effects of various parameters on the extraction efficiency of NSAIDs: (A) effect of HBD type; (B) effect of HBA: HBD molar ratio; (C) effect of DES volume; (D) effect of sample solution pH; (E) effect of PPF pore size; (F) effect of extraction time; (G) selection of desorption solvent; (H) effect of desorption time; and (I) effect of desorption solvent volume on peak intensity.

be hydrophobic partitioning of the neutral NSAID molecules into the hydrophobic DES phase, and that the highest extraction efficiencies would therefore be obtained under acidic conditions where the analytes (p*K*a ≈ 3–5) exist primarily in their protonated, neutral forms. Consistent with this expectation, relatively good extraction recovery was observed at low pH (2.0–4.0). However, as the pH was increased to 5.5—above the p*K*a of most studied NSAIDs, where a considerable fraction of the analytes become deprotonated and exist as anions—extraction recovery unexpectedly increased rather than decreased. This finding suggests that, in addition to hydrophobic partitioning, possible electrostatic interactions may contribute to the extraction process. The DES is composed of MTOAB, a quaternary ammonium salt with a permanently charged cationic center, and decanoic acid in a 1 : 3 molar ratio. While the abundant long alkyl chains provide a strongly hydrophobic matrix, the quaternary ammonium cation remains structurally intact and accessible, offering cationic sites for potential electrostatic interaction with anionic NSAIDs. The resulting synergistic effect, in which hydrophobic interactions serve as the primary retention mechanism and potential electrostatic attractions further enhance extraction, accounts for the improved recoveries observed at pH 5.5. At higher pH values, deprotonation of decanoic acid (saponification) may disrupt the hydrogen-bond network of the DES, leading to its decomposition or emulsification and a consequent decrease in extraction performance. Therefore, pH 5.5 was selected as the optimal condition.

3.4.3. Effect of ionic strength. To further investigate the influence of ionic strength on the extraction performance of the proposed method, NaCl was selected as the salt additive, and its concentration was varied from 0% to 5% (w/v). The addition of salt can alter the ionic strength of the sample solution and potentially affect the extraction efficiency through the salting-out effect. As shown in Fig. S1, the extraction recoveries of the target NSAIDs did not show a consistent improvement with increasing NaCl concentration. In some cases, a slight decrease in extraction efficiency was observed at higher salt levels, which may be attributed to the increased viscosity of the sample solution hindering mass transfer during the extraction process. Therefore, no NaCl was added in the subsequent experiments to simplify the procedure and maintain satisfactory extraction performance.

3.4.4. PPF pore size. The pore size of the PPF is a critical parameter determining the packing density of the fibers and the efficacy of DES immobilization, which could potentially influence the extraction equilibrium. To investigate this, PPFs with nominal pore sizes of 25, 50, 100, 150, and 300 μm were evaluated. SEM was employed to characterize the microstructure of the substrates. As illustrated in Fig. S2, the fibers across all PPF types exhibited similar morphology, characterized by smooth surfaces and consistent diameters. The primary distinction lay

in the fiber packing density: filters with smaller nominal pore sizes displayed significantly tighter fiber arrangements, whereas those with larger pore sizes featured looser networks.

The effect of these structural differences on extraction performance is shown in Fig. 4E. Interestingly, the extraction recoveries for the target analytes were comparable across all tested pore sizes, suggesting that the pore size did not significantly impact the efficiency of the DES-PPF-CME method. This phenomenon may be attributed to the excellent wettability and retention capability of the PPF for the DES, as well as the highly efficient mass transfer facilitated by the vigorous agitation (1000 rpm) employed in the current operation mode. The rapid convection generated during shaking likely minimizes the diffusion layer thickness, rendering the steric differences in pore size negligible. Although the extraction efficiency was similar, the 25 μm PPF was selected for subsequent experiments. Its denser fiber network may offer a higher retention capability, potentially ensuring better stability of the immobilized DES during the dynamic extraction process.

3.4.5. Extraction time. Extraction time is a critical parameter influencing the equilibrium and overall efficiency of the DES-PPF-CME method. Insufficient time may lead to incomplete mass transfer and lower sensitivity, while an excessively long duration limits sample throughput without yielding further improvements. Therefore, the extraction time was optimized over a range of 5 to 30 min.

As illustrated in Fig. 4F, the extraction recovery of the NSAIDs increased rapidly as the time was extended from 5 to 20 min, which was attributed to the efficient mass transfer of analytes from the aqueous phase to the DES phase. Beyond 20 min, the extraction recovery curves reached a plateau, indicating that the partition equilibrium had been established. To ensure maximum extraction efficiency while maintaining a practical analysis time, 20 min was selected as the optimal extraction time.

3.4.6. Desorption solvent type, volume, and time. The selection of an appropriate desorption solvent is crucial for efficiently releasing the target analytes from the DES phase. In this study, desorption was achieved by dissolving the DES containing the extracted analytes into an organic solvent compatible with the mobile phase, allowing for direct HPLC analysis without the need for evaporation or reconstitution.

The desorption efficiencies of four common solvents, including MeOH, EtOH, ACN, and acetone, were evaluated. As shown in Fig. 4G, ACN provided the highest enrichment factors for all analytes and demonstrated excellent reproducibility. Consequently, ACN was selected as the desorption solvent. The desorption time was also optimized over a range of 1 to 10 min. As illustrated in Fig. 4H, the extraction recovery reached a plateau after 3 min, indicating that this duration was sufficient for the quantitative desorption of the analytes.

Finally, the volume of the desorption solvent (0.1–1.0 mL) was optimized. Theoretically, a smaller desorption volume yields a higher analyte concentration, resulting in higher peak intensities. As shown in Fig. 4I, the peak intensities were indeed maximized at 0.1 mL. However, reducing the volume to 0.1 mL presents practical challenges, including difficulty in collecting the solution from the tube and poor reproducibility. Increasing the volume to 0.2 mL resulted in only a slight decrease in signal intensity but significantly improved the operational feasibility and reproducibility. Therefore, 0.2 mL of ACN was chosen as the optimal desorption volume for subsequent experiments.

3.5. Response surface optimization

To investigate the interactions among the key experimental variables and maximize the extraction efficiency, a three-factor, three-level RSM optimization was performed based on a Box–Behnken design (BBD). Design-Expert 12.0.3.0 software was used for the experimental design and statistical analysis. A total of 17 experimental runs were completed. Based on the single-factor experiments, the volume of DES (A), sample pH (B), and extraction time (C) were selected as independent variables, with the average recovery of the six NSAIDs as the response (Y) ($n = 3$). The experimental design and results are detailed in Tables S2 and S3.

The experimental data were fitted to a quadratic polynomial model, yielding the following regression equation:

$$Y = 72.72 + 5.65A - 4.07B - 5.9C + 2.62AB + 0.5250AC + 0.325BC - 6.55A^2 - 11.1B^2 - 5.45C^2$$

As shown in the ANOVA results (Table S4), the model is highly significant ($P < 0.01$), while the lack-of-fit term is non-significant ($P > 0.05$), indicating that the model accurately predicts the experimental data. The coefficient of determination (R^2) was 0.9912, and the adjusted R^2 (0.9799) was in close agreement with the predicted R^2, confirming a robust fit. The low coefficient of variation (CV = 2.3%) and high adequate precision (27.5) further attest to the model's reliability. Statistical analysis revealed that the linear terms (A, B, C), the interaction term (AB), and the quadratic terms (A^2, B^2, C^2) all significantly influenced the extraction recovery ($P < 0.01$).

Three-dimensional response surface plots (Fig. 5) were generated to visualize the interactions between variables. Notably, the interaction between DES volume and sample pH (Fig. 5A) exhibited a steep surface with dense contour lines, signifying a strong synergistic effect on extraction efficiency. In contrast, the interactions between DES volume and extraction time (Fig. 5B) or pH and extraction time (Fig. 5C) were less pronounced.

The optimal conditions predicted by the model were 18.015 μL of DES, a sample pH of 5.335, and an extraction time of 22.294 min. For experimental feasibility, these parameters were adjusted to 18 μL of DES, pH 5.3 and extraction time of 22 min. Verification experiments ($n = 4$) conducted under these conditions yielded extraction recoveries consistent with the predicted values (deviation < 0.5%), confirming the validity and practical applicability of the optimized DES-PPF-CME method.

3.6. Performance of DES-PPF-CME device for storage

To further evaluate the storage stability and practical applicability of the DES-PPF-CME device, the performance of the prepared extraction devices after long-term storage was

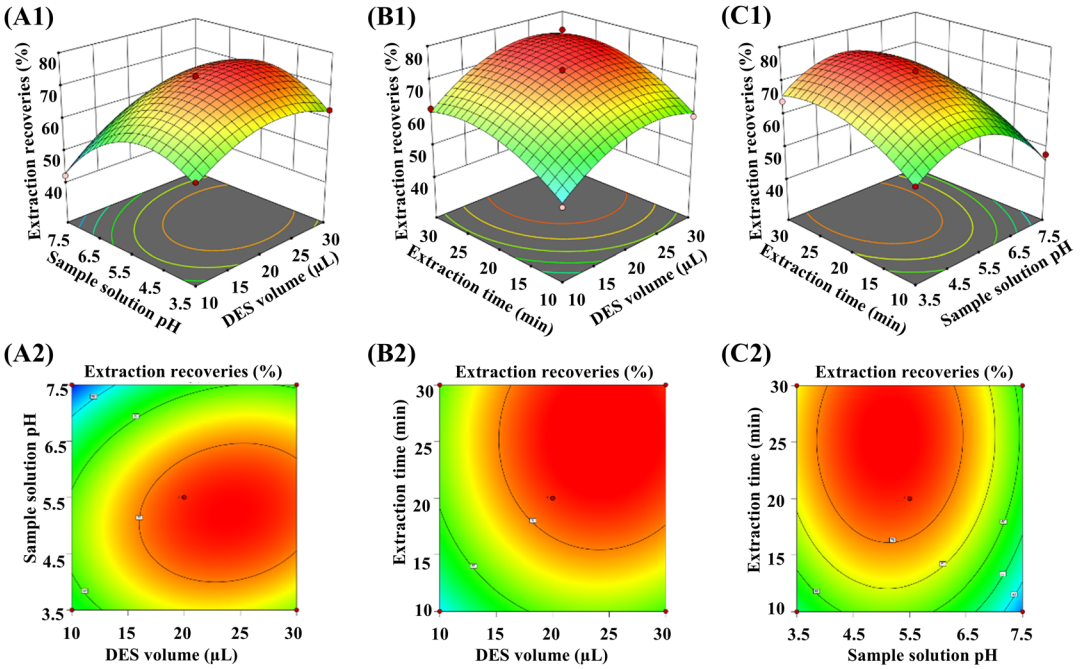

Fig. 5 Response surface (3D) and contour (2D) plots illustrating the effects of key parameters on the extraction recovery of NSAIDs: (A) interaction between sample pH and DES volume, (B) interaction between extraction time and DES volume, and (C) interaction between extraction time and sample pH.

investigated. After fabrication, the DES-PPF-CME devices were sealed in plastic bags and stored at room temperature. The stored devices were tested after 1, 2, and 3 months under the same extraction conditions, and their extraction efficiencies toward the target NSAIDs were compared with those of freshly prepared devices. As shown in Fig. S3, no significant differences in extraction efficiency were observed among the devices stored for different periods. The results indicate that the DES-PPF-CME device can maintain its structural integrity and extraction performance for at least three months under ambient storage conditions. This stability is attributed to the good compatibility between the hydrophobic DES and the polypropylene fabric matrix, as well as the inherent chemical stability of both materials. These findings demonstrate the excellent storage stability of the DES-PPF-CME device and further support its feasibility as a ready-to-use extraction tool for routine analytical applications.

To visually examine whether the DES would detach from the PPF support during the extraction process, a simple visualization experiment was conducted. Because the synthesized DES is a light-yellow liquid and difficult to observe directly, a small amount of Oil Red O was added to the DES to produce a dark red color. As shown in Fig. S4, the sample solution remained colorless both before and after extraction under the optimized conditions, indicating that the DES did not leach into the sample solution during the extraction process. Meanwhile, the colored DES on the PPF exhibited only further diffusion within the pores of the fabric after extraction. These observations suggest that the DES was firmly immobilized on the PPF matrix and no noticeable detachment occurred during the extraction process, confirming the stability of the DES-PPF-CME device.

To provide quantitative evidence, the mass change of the DES-PPF device was determined before and after extraction. Because residual sample solution could affect gravimetric measurements, the devices were freeze-dried prior to weighing. The result showed that the relative mass change of DES-PPF after extraction and freeze-drying ranged from −1.02% to −0.20%, indicating no significant mass loss during the extraction process. Collectively, these results confirm that DES leaching is negligible and that the interaction between DES and the PPF support remains highly stable under routine extraction.

To further evaluate the reproducibility of the fabricated extraction devices, the batch-to-batch variation was investigated. Five independent batches of DES-PPF-CME devices were prepared, and the target analytes in the samples were extracted using the same procedure. As illustrated in Fig. S5, only minor variations in extraction performance were observed among the different batches. These results demonstrate good fabrication reproducibility of the devices and indicate that the prepared DES-PPF-CME devices possess satisfactory batch-to-batch consistency.

3.7. Method validation

The analytical performance of the proposed DES-PPF-CME method was evaluated under the optimized conditions. Key validation parameters, including linearity, R^2, limits of detection (LODs), and limits of quantification (LOQs), are summarized in Table 1. Calibration curves were constructed using six concentration levels for each analyte. The exact concentrations used for calibration were as follows: SLD and DCF, 50, 100, 200, 300, 400, and 500 ng mL^{-1}; LOX and IBU, 80, 160, 320, 480, 640, and 800 ng mL^{-1}; FBP, 20, 80, 160, 320, 480, and 800 ng mL^{-1};

Table 1 Linear ranges, regression data, LODs and LOQs for the determination of NSAIDs

Analyte	Linear range (ng mL^{-1})	Slope ± SE	Intercept ± SE	R^2	RSS	LOD (ng mL^{-1})	LOQ (ng mL^{-1})
SLD	50–800	0.0864 ± 0.0023	−0.5561 ± 0.5945	0.9960	3.4771	9.1	30.2
LOX	80–800	0.0398 ± 0.0016	−0.5301 ± 0.3675	0.9839	1.1043	19.7	65.7
NPX	5–800	0.4983 ± 0.0047	0.0578 ± 0.9880	0.9994	31.3252	1.1	3.8
FBP	20–800	0.1280 ± 0.0048	−0.3336 ± 1.0849	0.9856	23.9425	4.9	16.2
DCF	50–800	0.0553 ± 0.0012	−0.4866 ± 0.2119	0.9985	0.8579	13.1	43.7
IBU	80–800	0.0550 ± 0.0027	−0.4901 ± 0.6575	0.9915	2.7993	13.7	45.8

NPX, 5, 20, 80, 160, 400, and 800 ng mL^{-1}. All analytes showed good linearity, with R^2 exceeding 0.9839. The LODs and LOQs were determined to be in the ranges of 1.1–19.7 ng mL^{-1} and 3.8–65.7 ng mL^{-1}, respectively, indicating high sensitivity suitable for trace analysis. Previous pharmacokinetic studies have reported that the peak plasma concentrations (C_{max}) of these NSAIDs generally fall within the μg mL^{-1} range. For example, the reported C_{max} values are ~7.4 μg mL^{-1} for sulindac,[21] ~7.2 μg mL^{-1} for loxoprofen,[22] and ~14–19 μg mL^{-1} for flurbiprofen[23] after therapeutic oral administration. Therefore, plasma samples with concentrations exceeding the calibration range can be appropriately diluted before analysis.

To assess the accuracy and precision of the method, intra-day and inter-day relative recovery experiments were conducted at three different concentration levels. As detailed in Table S4 and illustrated in Fig. 6A and B, the relative recoveries ranged from 87.3% to 109.8%, demonstrating satisfactory accuracy. The precision was also robust, with intra-day relative standard deviations (RSDs) ranging from 0.4% to 7.1% and inter-day RSDs ranging from 1.4% to 8.6%. These results confirm that the developed method is reliable and reproducible for the quantitative analysis of NSAIDs.

3.8. Matrix influence

The influence of the plasma matrix on analyte determination was evaluated by comparing the slopes of calibration curves prepared in pure solvent and in matrix-matched samples. The effect was calculated based on the ratio of the slope of the matrix-matched calibration curve to that of the pure solvent calibration curve, using the following equation.[24]

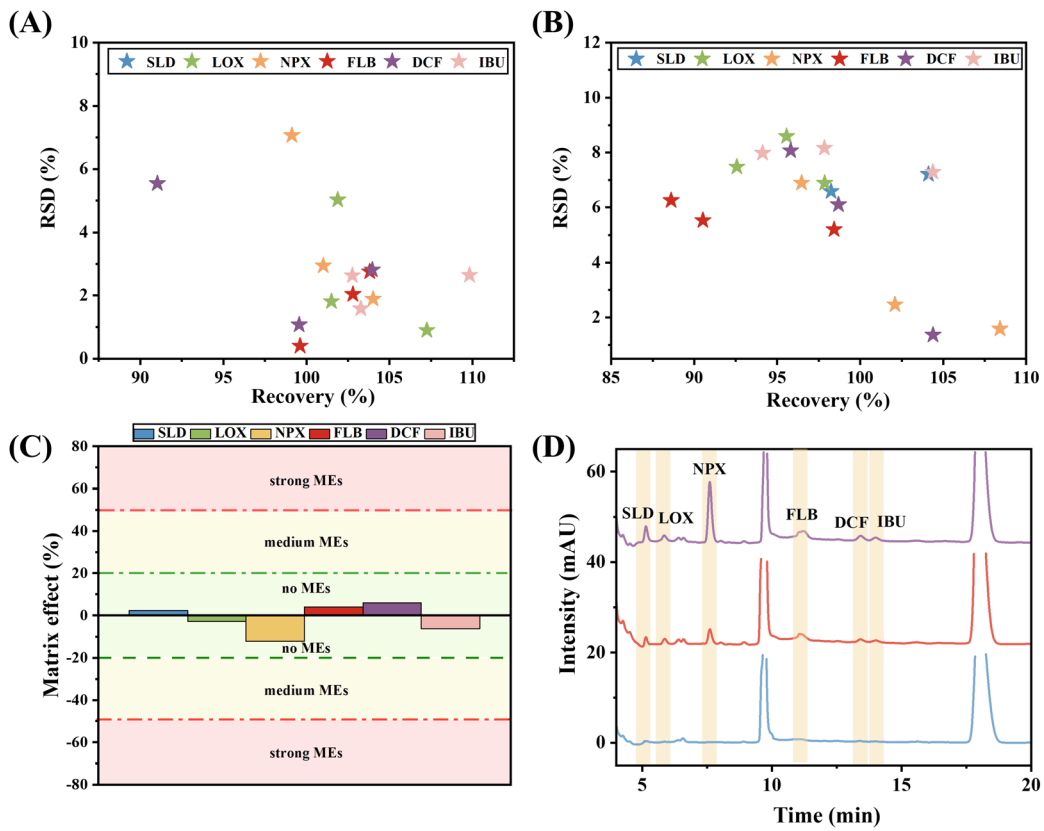

Fig. 6 Performance evaluation of the DES-PPF-CME method: (A) intra-day precision and accuracy, (B) inter-day precision and accuracy, (C) matrix influence, and (D) representative HPLC-UV chromatograms of (a) blank plasma, (b) plasma spiked at low concentrations (SLD, LOX, DCF, IBU, FBP at 200 ng mL^{-1}; NPX at 100 ng mL^{-1}), and (c) plasma spiked at high concentrations (500 ng mL^{-1} for all analytes).

$$\mathrm{ME}(\%) = \left(\frac{\text{slope of matrix calibration curves}}{\text{slope of pure solvent calibration curves}} - 1\right) \times 100\%$$

Calibration curves in pure solvent were prepared by diluting NSAID stock solutions with deionized water, while matrix-matched calibration curves were obtained using processed blank plasma samples. The calculated effects were classified as weak ($|ME| \leq 20\%$), medium ($20\% < |ME| \leq 50\%$), or strong ($|ME| > 50\%$), with weak MEs considered negligible.[25] As shown in Fig. 6C, the calculated values ranged from −12.2% to 5.9%. These results indicate that the plasma matrix exerted minimal influence on the analytical response of the target analytes, suggesting that external standard calibration can be applied.

3.9. Sample analysis

Due to ethical restrictions, real patient plasma samples were not available for the present study. Therefore, drug-free plasma samples spiked with known concentrations of the analytes were used to evaluate the feasibility of the proposed method in a complex biological matrix. To minimize analytical bias, the spiking levels were prepared independently, and the nominal concentrations were disclosed only after all measurements had been finalized.[26,27]

The results showed that at spiking levels of 200 and 500 ng mL^{-1}, all six NSAIDs were successfully detected in plasma using the DES-PPF-CME method, with spike recoveries ranging from 88.8% to 105.8%. All experiments were performed in triplicate ($n = 3$), and the mean values are reported. Detailed results are summarized in Table S6, and representative HPLC chromatograms of blank and spiked plasma samples are shown in Fig. 6D. The chromatograms of blank plasma showed no detectable signals, indicating that endogenous components did not interfere with the determination of the target analytes.

To further assess the influence of individual matrix variability, the extraction and analysis were performed on each of the six plasma samples that were originally pooled. Each individual plasma sample was spiked with the target NSAIDs at the same concentration level and processed under the optimized conditions. The relative recoveries for all analytes across the six individual sources ranged from 80% to 120%, confirming that the method is not significantly affected by inter-individual differences in plasma composition and provides acceptable accuracy for the analysis of clinical specimens. The detailed results are presented in Fig. S6.

It should be noted that HPLC-UV was employed in this study due to its robustness and wide availability, providing adequate sensitivity and selectivity for the spiked samples. For applications requiring higher selectivity and sensitivity, the DES-PPF-CME strategy can be readily coupled with HPLC-MS/MS and further established under rigorous bioanalytical validation for potential clinical applications.

3.10. Method comparison

The analytical performance and operational characteristics of the proposed DES-PPF-CME method were compared with previously reported techniques for NSAID determination. The critical distinguishing feature of the DES-PPF-CME method is that the extraction phase is pre-assembled into the cap, rendering the entire device a disposable, no-assembly-required unit. This cap-type format enables true batch processing by simple shaking, which to the best of our knowledge has not been reported for supported liquid membrane extraction of NSAIDs in biofluids. As summarized in Table S7, the comparison considers three main aspects: operational simplicity and throughput, environmental impact, and overall analytical performance.

Firstly, the proposed method introduces a ready-to-use extraction device in which the DES-immobilized polypropylene fabric (PPF) phase is pre-integrated into the cap of a centrifuge tube. This configuration simplifies the sample preparation workflow: extraction, phase separation between the DES and the sample solution, and desorption can all be completed through simple tube inversion and agitation. Consequently, the procedure is compatible with batch processing and potential automation, allowing multiple samples (*e.g.*, 24 tubes or more) to be processed simultaneously without complex manual operations. This differs from most DES-assisted microextraction approaches (*e.g.*, AALLME,[28] UA-DLLME[29]), which typically rely on centrifugation for phase separation followed by manual collection of the extractant. It also differs from conventional polypropylene/fabric-based extraction supports (*e.g.*, PF-SPE[30]), which generally require multiple vortexing and centrifugation steps. The elimination of centrifugation and simplified handling may therefore improve operational convenience in high-throughput laboratory settings.

Secondly, the environmental performance of the proposed method was evaluated using the AGREE metric. The AGREE score was derived by transforming 12 input variables (each reflecting a principle of green analytical chemistry) to a common 0–1 scale and assigning them individual weights according to their perceived importance. The weighted scores were then combined to yield an overall score between 0 and 1, which is displayed together with a clock-like graph with a color code at the center. In this evaluation, the DES-PPF-CME method received high scores in aspects related to waste, sample throughput, and operator safety (principles 2, 4, 6, 11, 12), whereas lower scores were obtained for principles such as sample preparation and energy consumption (principles 1, 3, 10), and achieved an AGREE score of 0.74, which is slightly higher than those reported for the compared methods (0.48–0.72). This result can be attributed to several factors, including the use of a low-volatility DES as the extraction solvent, the avoidance of centrifugation or vacuum-assisted procedures, and the relatively small solvent consumption per analysis. These characteristics suggest that the method is consistent with the general principles of green analytical chemistry.

Thirdly, in terms of analytical performance, the DES-PPF-CME method provides relative recoveries of 87.3–108.4% and limits of detection of 1.1–19.7 ng mL^{-1}. These figures of merit are comparable to those reported for several previously published methods. For example, the LODs are lower than those

obtained using SPE-UPLC-UV (15.7–23.6 ng mL^{-1})[31] and comparable to AALLME (0.3–0.9 ng mL^{-1})[28] and PF-SPE (0.3–1.0 ng mL^{-1}),[30] despite the use of a conventional UV detector in the present study. In addition, the materials used in the DES-PPF-CME device, including the DES components and the polypropylene fabric support, are inexpensive and easy to fabricate, which may facilitate potential large-scale preparation of the extraction devices.

It should also be noted that acetonitrile-based protein precipitation is widely used for plasma sample preparation prior to HPLC-UV analysis. While this approach is operationally straightforward, it generally requires centrifugation and manual collection of the supernatant. In contrast, the DES-PPF-CME format integrates the extraction phase into a disposable cap device and enables centrifugation-free operation through simple shaking steps. This configuration may offer advantages in terms of simplified handling and parallel processing when multiple samples are analyzed.

Overall, the proposed DES-PPF-CME strategy combines acceptable analytical performance with operational simplicity and relatively favorable environmental characteristics, suggesting that it may serve as a practical sample preparation platform for microextraction-based analysis.

4. Conclusion

In this work, a facile, cost-effective, and operator-friendly sample preparation strategy, termed DES-PPF-CME, was successfully developed for the sensitive determination of NSAIDs in plasma. By immobilizing a hydrophobic DES onto a polypropylene fabric substrate within a disposable tube cap, a distinctive 'ready-to-use' extraction device was introduced, representing a new format of supported liquid membrane extraction. This design uniquely enables a simplified workflow: extraction, phase separation between the DES and sample solution, and desorption are accomplished through simple tube inversion and vortexing. Consequently, the process becomes readily amenable to automation and high-throughput batch processing. This stands in contrast to most DES-assisted microextraction methods, which typically rely on centrifugation for phase separation followed by manual collection of the extractant, as well as to conventional polypropylene/fabric-based extraction supports that often necessitate manual intervention and pose challenges for automation. Under the conditions optimized *via* Box–Behnken design, the method demonstrated good analytical performance, characterized by low limits of detection (1.1–19.7 ng mL^{-1}), satisfactory precision (RSDs < 8.6%), and high relative recoveries (88.8–105.8%) in spiked plasma samples. In summary, the cap-type extraction device introduced herein represents a distinct advance in supported liquid membrane extraction, as it converts the typically labor-intensive, centrifugation-dependent workflow into a streamlined, shake-and-inject procedure directly compatible with batch processing and potential automation. Future studies can focus on applying this strategy to real clinical plasma samples and conducting more comprehensive bioanalytical validation according to regulatory guidelines to facilitate its subsequent clinical application.

Ethical approval

All experiments involving human blood samples were performed in accordance with the Declaration of Helsinki, relevant national regulations, and institutional guidelines, and were approved by the Ethics Committee of the Second Affiliated Hospital of Zhengzhou University. Informed consent was obtained from all human participants involved in this study.

Conflicts of interest

The authors declare that they have no competing interests.

Data availability

All data underlying the results are available as part of the article and no additional source data is required.

Supplementary information (SI): additional figures (Fig. S1–S6), and tables (Tables S1–S7). See DOI: https://doi.org/10.1039/d6ra02568d.

Acknowledgements

This work was supported by the National Natural Science Foundation of China (Grant No. 8240081392), and Henan Provincial Science and Technology Research Project (Grant No. 262102311173).

References

1 A. Rodriguez-Miguel, L. A. Garcia-Rodriguez, M. Gil, D. Barreira-Hernandez, S. Rodriguez-Martin and F. J. de Abajo, *Aliment. Pharmacol. Ther.*, 2019, **50**, 295, DOI: 10.1111/apt.15333.
2 Z. Zhang, H. Xu, Y. Zhang, W. Li, Y. Yang, T. Han, Z. Wei, X. Xu and J. Gao, *J. Clin. Anesth.*, 2017, **43**, 84, DOI: 10.1016/j.jclinane.2017.08.030.
3 Y. G. Cao, M. Zhang, D. Yu, J. P. Shao, Y. C. Chen and X. Q. Liu, *Anal. Bioanal. Chem.*, 2008, **391**, 1063, DOI: 10.1007/s00216-008-2054-4.
4 S. Peng, X. Huang, Y. Huang, Y. Huang, J. Zheng, F. Zhu, J. Xu and G. Ouyang, *J. Sep. Sci.*, 2022, **45**, 282, DOI: 10.1002/jssc.202100634.
5 M. E. I. Badawy, M. A. M. El-Nouby, P. K. Kimani, L. W. Lim and E. I. Rabea, *Anal. Sci.*, 2022, **38**, 1457, DOI: 10.1007/s44211-022-00190-8.
6 E. Olvera-Urena, B. Aguilar-Perez, K. A. Escamilla-Lara, J. Lopez-Tellez, S. Ramirez-Montes and J. A. Rodriguez, *Crit. Rev. Anal. Chem.*, 2025, 1–25, DOI: 10.1080/10408347.2025.2527758.
7 S. Hamidi, N. Alipour-Ghorbani and A. Hamidi, *Crit. Rev. Anal. Chem.*, 2018, **48**, 239, DOI: 10.1080/10408347.2017.1396885.

8 W. Mo, L. Li, B.-C. Yang, X. Wang, B. Wang, J. Zhang, Q. Huang, Z.-P. Yao, D. Zhang and B. Hu, *Anal. Chim. Acta*, 2024, **1318**, 342923, DOI: 10.1016/j.aca.2024.342923.
9 J. Yan, J. Huang, S. Peng, D. Sun, W. Lu, Z. Song, J. Ma, J. You, H. Fan and L. Chen, *J. Chromatogr. A*, 2025, **1754**, 466016, DOI: 10.1016/j.chroma.2025.466016.
10 J. Bintanel-Cenis, M. A. Fernandez, B. Gomara and L. Ramos, *Talanta*, 2024, **270**, 125599, DOI: 10.1016/j.talanta.2023.125599.
11 A. A. Lemos, A. L. Chapana, C. E. Lujan, M. B. Botella, M. N. Oviedo and R. G. Wuilloud, *Anal. Bioanal. Chem.*, 2025, **417**, 1239, DOI: 10.1007/s00216-024-05578-1.
12 T. N. Huynh, T. T. Nguyen, C. D. Tran, Q. T. Nguyen, H. T. Nguyen, A. D. Trinh and Q. H. Tran, *J. Mol. Liq.*, 2025, **422**, 126954, DOI: 10.1016/j.molliq.2025.126954.
13 S. Shokouh, S. M. Daryanavard, F. M. Suzaei, A. Fuente-Ballesteros and C. Saenjum, *Green Anal. Chem.*, 2025, **15**, 100296, DOI: 10.1016/j.greeac.2025.100296.
14 Y. Wang, J. Li, D. Sun, S. Yang, H. Liu and L. Chen, *J. Chromatogr. A*, 2021, **1658**, 462615, DOI: 10.1016/j.chroma.2021.462615.
15 E. Carasek, G. Bernardi, D. Morelli and J. Merib, *J. Chromatogr. A*, 2021, **1640**, 461944, DOI: 10.1016/j.chroma.2021.461944.
16 P. Makoś, E. Słupek and J. Gębicki, *Microchem. J.*, 2020, **152**, 104384, DOI: 10.1016/j.microc.2019.104384.
17 Y. Wang, M. Lv, Y. Liu, X. Xia, N. Zhang and D. Chen, *Biomed. Anal.*, 2025, **2**, 120, DOI: 10.1016/j.bioana.2025.09.003.
18 Y. Wang, M. Lv, Y. Liu, X. Xia, N. Zhang and D. Chen, *Biomed. Anal.*, 2025, **2**, 120, DOI: 10.1016/j.bioana.2025.09.003.
19 R. Ahmadi, G. Kazemi, A. M. Ramezani and A. Safavi, *Microchem. J.*, 2019, **145**, 501, DOI: 10.1016/j.microc.2018.11.005.
20 W.-C. Han, H.-J. Zhang, J.-B. Chen, Y.-Y. Chen, W.-J. Wang, Y.-W. Liu, P. Yang, D.-D. Yuan and D. Chen, *J. Mol. Liq.*, 2024, **395**, 123875, DOI: 10.1016/j.molliq.2023.123875.
21 W. H. Huang, L. Shao, S. X. Li, D. Guo, L. S. Wang, Z. Li and Z. R. Tan, *Anal. Methods*, 2014, **6**(13), 4679, DOI: 10.1039/c4ay00730a.
22 K. Adachi, Y. Sugitani, R. Unita, K. Yoshida, S. Beppu, M. Terashima, M. Fujii, M. Shimizu and H. Yamazaki, *J. Pharm. Health Care Sci.*, 2021, **7**, 33, DOI: 10.1186/s40780-021-00216-9.
23 L. Ozbay, D. O. Unal, I. Cakici, A. Fenercioglu and D. Erol, *Eur. J. Drug Metab. Pharmacokinet.*, 2009, **34**(1), 1, DOI: 10.1007/bf03191376.
24 P. Garcia-Atienza, H. Martinez-Perez-Cejuela, J. Manuel Herrero-Martinez and S. Armenta, *Talanta*, 2024, **267**, 125277, DOI: 10.1016/j.talanta.2023.125277.
25 N. Besil, V. Cesio, H. Heinzen and A. R. Fernandez-Alba, *J. Agric. Food Chem.*, 2017, **65**, 4819, DOI: 10.1021/acs.jafc.7b00243.
26 C. Bottinelli, R. Nicoli, F. Bevalot, N. Cartiser, C. Roger, K. Chikh, T. Kuuranne, L. Fanton and J. Guitton, *Talanta*, 2021, **225**, 122047, DOI: 10.1016/j.talanta.2020.122047.
27 D. Wang, M. Li, T. Dai, X. Zhang and D. Chen, *J. Chromatogr. A*, 2025, **1760**, 466315, DOI: 10.1016/j.chroma.2025.466315.
28 M. Bazregar, M. Rajabi, Y. Yamini, A. Asghari and M. Hemmati, *Anal. Chim. Acta*, 2016, **917**, 44, DOI: 10.1016/j.aca.2016.03.005.
29 L. Qiao, R. Sun, C. Yu, Y. Tao and Y. Yan, *Microchem. J.*, 2021, **170**, 106686, DOI: 10.1016/j.microc.2021.106686.
30 N. Moradi, G. Soufi, A. Kabir, M. Karimi and H. Bagheri, *Anal. Chim. Acta*, 2023, **1270**, 341461, DOI: 10.1016/j.aca.2023.341461.
31 A. Alhendal, *RSC Adv.*, 2025, **15**, 9364, DOI: 10.1039/d5ra00253b.